

I κ B Kinase α/β Control Biliary Homeostasis and Hepatocarcinogenesis in Mice by Phosphorylating the Cell-Death Mediator Receptor-Interacting Protein Kinase 1

Christiane Koppe,¹ Patricia Verheugd,² Jérémie Gautheron,¹ Florian Reisinger,³ Karina Kreggenwinkel,¹ Christoph Roderburg,¹ Luca Quagliata,⁴ Luigi Terracciano,⁴ Nikolaus Gassler,⁵ René H. Tolba,⁶ Yannick Boege,⁷ Achim Weber,⁷ Michael Karin,⁸ Mark Luedde,⁹ Ulf P. Neumann,¹⁰ Ralf Weiskirchen,¹¹ Frank Tacke,¹ Mihael Vucur,¹ Christian Trautwein,¹ Bernhard Lüscher,² Christian Preisinger,¹² Mathias Heikenwalder,^{3,13*} and Tom Luedde^{1*}

The I κ B-Kinase (IKK) complex—consisting of the catalytic subunits, IKK α and IKK β , as well as the regulatory subunit, NEMO—mediates activation of the nuclear factor κ B (NF- κ B) pathway, but previous studies suggested the existence of NF- κ B-independent functions of IKK subunits with potential impact on liver physiology and disease. Programmed cell death is a crucial factor in the progression of liver diseases, and receptor-interacting kinases (RIPKs) exerts strategic control over multiple pathways involved in regulating novel programmed cell-death pathways and inflammation. We hypothesized that RIPKs might be unrecognized targets of the catalytic IKK-complex subunits, thereby regulating hepatocarcinogenesis and cholestasis. In this present study, mice with specific genetic inhibition of catalytic IKK activity in liver parenchymal cells (LPCs; IKK α/β ^{LPC-KO}) were intercrossed with RIPK1^{LPC-KO} or RIPK3^{-/-} mice to examine whether RIPK1 or RIPK3 might be downstream targets of IKKs. Moreover, we performed *in vivo* phospho-proteome analyses and *in vitro* kinase assays, mass spectrometry, and mutagenesis experiments. These analyses revealed that IKK α and IKK β —in addition to their known function in NF- κ B activation—directly phosphorylate RIPK1 at distinct regions of the protein, thereby regulating cell viability. Loss of this IKK α/β -dependent RIPK1 phosphorylation in LPCs inhibits compensatory proliferation of hepatocytes and intrahepatic biliary cells, thus impeding HCC development, but promoting biliary cell paucity and lethal cholestasis. **Conclusions:** IKK-complex subunits transmit a previously unrecognized signal through RIPK1, which is fundamental for the long-term consequences of chronic hepatic inflammation and might have potential implications for future pharmacological strategies against cholestatic liver disease and cancer. (HEPATOLOGY 2016;64:1217-1231)

Whereas in most instances, hepatocellular carcinoma (HCC) arises in a setting of chronic inflammation and subsequent liver fibrosis, anti-inflammatory pharmacological strategies have not yet entered clinical practice for prevention or treatment of HCC.⁽¹⁾ The nuclear

Abbreviations: ALT, alanine aminotransferase; AP, alkaline phosphatase; CK, cytokeratin; cl. CASP-3, cleaved CASPASE-3; EMSA, electrophoretic mobility shift assay; FADD, Fas-associated protein with death domain; floxed, loxP-site-flanked; GAPDH, glyceraldehyde-3-phosphate dehydrogenase; GFP, green fluorescent protein; HA, hemagglutinin; HCC, hepatocellular carcinoma; HSP-90, heat shock protein 90; IKK, I κ B kinase; IHC, immunohistochemical staining; LPCs, liver parenchymal cells; LPC-KO, liver parenchymal cell-specific knockout; LPS, lipopolysaccharide; MTT, methyl thiazol tetrazolium; Nec-1, necrostatin 1; NF- κ B, nuclear factor κ B; qRT-PCR, quantitative real-time polymerase chain reaction; RIPK1, receptor-interacting protein-kinase-1; RIPK3, receptor-interacting-protein-kinase-3; TPCA-1, thiophenecarboxamide; TNF, tumor necrosis factor; TNFR1, TNF receptor 1; TRADD, TNFR1-associated DEATH domain; WT, wild type.

Received December 1, 2015; accepted July 1, 2016.

Additional Supporting Information may be found at onlinelibrary.wiley.com/doi/10.1002/hep.28723/suppinfo.

factor κ B (NF- κ B) pathway contributes to the pathophysiology of inflammation.⁽²⁾ Activation of NF- κ B in response to cytokines like tumor necrosis factor (TNF) relies on a high-molecular-weight complex, the I κ B kinase (IKK) complex, consisting of two catalytic subunits—IKK α (IKK1) and IKK β (IKK2)—and a regulatory subunit called NEMO (IKK γ).⁽³⁾ Though recently alternative, NF- κ B-independent functions of IKK subunits were suggested *in vitro*,^(4,5) the nature and relevance of the latter *in vivo* and, especially, in inflammation and carcinogenesis have remained elusive.

The receptor-interacting protein kinase 1 (RIPK1/RIP1) exerts strategic control over multiple pathways involved in regulating inflammation and cell death.⁽⁶⁾ It was suggested to promote necroptosis, a novel form of programmed necrosis—by assembling with RIPK3.⁽⁷⁻⁹⁾ In addition, the presence and activation status of RIPK1 define two distinct forms of apoptosis.⁽¹⁰⁾ TNF receptor 1 (TNFR1)-dependent recruitment of TNFR1-

associated DEATH domain (TRADD) leads to formation of complex IIA, mediates apoptosis independently of RIPK1, and counterbalanced by NF- κ B activation through the NF- κ B target-gene, c-FLIP.⁽¹¹⁾ An alternative, RIPK1-dependent complex, IIB, proceeds independently of TRADD through a RIPK1/FADD (Fas-associated protein with death domain) scaffold to activate CASPASE-8.⁽¹¹⁾ Importantly, these distinct apoptosis pathways and signaling platforms have mainly been defined in cell-culture studies.^(10,11) The function of RIPK1 in liver biology and disease is not well defined and a matter of intense recent debate.^(12,13) Though previous studies focused on the role of RIPK1 in hepatic injury,⁽¹²⁻¹⁴⁾ it is presently unknown whether RIPK1 plays a functional role in regulation of chronic liver disease (e.g., cancer development). Moreover, it is not well defined how RIPK-dependent cell-death pathways like apoptosis and necroptosis functionally interact with NF- κ B-related survival signals, which was examined in the present study.

Work in the lab of T.L. was supported by a Mildred Scheel Endowed Professorship and a single project grant (110043) from the German Cancer Aid (Deutsche Krebshilfe), the German Research Foundation (LU 1360/3-1 and SFB-TRR57/P06), an ERC Starting Grant (ERC-2007-Sig I 208237-Luedde-Med3-Aachen), the EMBO Young Investigator Program, the Interdisciplinary Center for Clinical Research (IZKF) Aachen, Germany, the Ernst-Jung-Foundation Hamburg, and a grant from the medical faculty of the RWTH Aachen. M.H. was supported by the Helmholtz Foundation, the Hofschneider Foundation, the German Research Foundation (SFB-TR36), the Helmholtz Alliance PCCC, and an ERC Starting grant (LiverCancerMechanisms). B.L. was supported by the German Research Foundation (LU 466/16-1) and the Interdisciplinary Center for Clinical Research (IZKF) Aachen, Germany. The Proteomics Facility (C.P.) is supported by the Interdisciplinary Center for Clinical Research (IZKF) Aachen, Germany. M.L. was supported by the Deutsche Stiftung Herzforschung (12/12). Mouse strain generation and breeding in M.K.'s lab was supported by the NIH (R01 AI043477).

**These authors contributed equally to this work.*

Copyright © 2016 by the American Association for the Study of Liver Diseases.

View this article online at wileyonlinelibrary.com.

DOI 10.1002/hep.28723

Potential conflict of interest: Nothing to report.

ARTICLE INFORMATION:

From the ¹Department of Medicine III, Division of Gastroenterology, Hepatology and Hepatobiliary Oncology, University Hospital RWTH Aachen, Aachen, Germany; ²Institute of Biochemistry and Molecular Biology, University Hospital RWTH Aachen University, Aachen, Germany; ³Department of Virology, Technische Universität München/Helmholtz Zentrum München für Gesundheit und Umwelt (HMGU), Munich, Germany; ⁴Institute of Pathology, University Hospital of Basel, Basel, Switzerland; ⁵Institute of Pathology, Hospital of Braunschweig, Braunschweig, Germany; ⁶Department of Laboratory Animal Research, University Hospital RWTH Aachen, Aachen, Germany; ⁷Institute of Surgical Pathology, University Hospital Zurich, Zurich, Switzerland; ⁸Department of Pharmacology and Pathology, School of Medicine, UCSD, La Jolla, CA; ⁹Department of Cardiology and Angiology, University Hospital Schleswig-Holstein, Kiel, Germany; ¹⁰Department of Visceral and Transplantation Surgery University Hospital RWTH Aachen, Aachen, Germany; ¹¹Institute of Molecular Pathobiochemistry, Experimental Gene Therapy and Clinical Chemistry University Hospital RWTH Aachen, Aachen, Germany; ¹²Proteomics Facility, Interdisciplinary Center for Clinical Research (IZKF) Aachen, University Hospital RWTH Aachen, Aachen, Germany; ¹³Division of Chronic Inflammation and Cancer, German Cancer Research Center (DKFZ), Heidelberg, Germany.

ADDRESS CORRESPONDENCE AND REPRINT REQUESTS TO:

Tom Luedde, M.D., Ph.D.
Mildred-Scheel-Professor for Gastroenterology
Hepatology and Hepatobiliary Oncology
Medical Clinic III, University Hospital RWTH Aachen

Pauwelsstrasse 30
D-52074 Aachen, Germany
E-mail: tluedde@ukaachen.de
Tel: +49-241-8080865

Materials and Methods

GENERATION OF GENETICALLY MODIFIED MOUSE MODELS

NEMO^{LPC-KO} mice were generated as described.⁽¹⁵⁾ Mice carrying loxP-site-flanked (floxed) alleles of *Ikkα/Ikkβ* (IKK^{FL}),⁽¹⁶⁾ *Ikkβ/Ikkβ* (IKK^{FL})⁽¹⁷⁾ were crossed to Alfp-Cre transgenic mice⁽¹⁸⁾ to generate a liver parenchymal cell (LPC)-specific knockout (LPC-KO) of the respective genes. Mice with double knockout of *Ikkα/Ikkβ* (IKK^{α/β}^{LPC-KO}) in LPCs were generated by intercrossing the respective lines. For generation of IKK^{AA/AA}/IKK^β^{LPC-KO} mice, IKK^β^{LPC-KO} mice were crossed to IKK^α^{AA/AA} knock-in mice in which the activating phosphorylation sites of IKK^α, Ser176, and Ser180 were replaced by alanines.⁽¹⁹⁾ Mice with combined constitutive *Ripk3*-deletion (RIPK3^{-/-})⁽²⁰⁾ and conditional *Ikkα/Ikkβ* deletion (IKK^{α/β}^{LPC-KO}/RIPK3^{-/-}) were generated by intercrossing the respective lines. Mice with triple knockout of *Ikkα/Ikkβ/Ripk1* (IKK^{α/β}/RIPK1^{LPC-KO}) were generated by intercrossing RIPK1^{FL} mice⁽¹³⁾ with IKK^{α/β}^{LPC-KO} mice.

In all experiments, littermates carrying the respective loxP-flanked alleles, but lacking expression of Cre recombinase, were used as wild-type (WT) controls. Mice were bred on a mixed C57/BL6xSV129Ola genetic background. Only sex-matched animals were compared. Unless otherwise indicated, mice were analyzed at 7–9 weeks of age. Animals received human care according to European, national, and institutional regulations.

HUMAN LIVER TISSUE

Human liver biopsy specimens and clinicopathological data were obtained from the Institute of Pathology, University Hospital Aachen, and the Institute of Pathology, University Hospital Basel. The project was authorized by the local ethics committees and conducted in accord with the ethical standards laid down in the Declaration of Helsinki (ethics committee of the University Hospital of Aachen, Germany [reference no.: EK 206/09] and ethics committee of the University Hospital of Basel, Switzerland [reference no.: EK 310/12]). Histological grading and staging was performed according to the World Health Organization classification of tumors of the digestive system (2010).

STATISTICAL ANALYSIS

Results are expressed as the mean + SEM. The significance of differences between groups was assessed using an unpaired two-sample *t* test. Survival curves were generated using the Kaplan-Meier method, and the significance of the difference in survival rate was determined by the log-rank test (GraphPad Prism; GraphPad Software Inc., La Jolla, CA). Correlation analysis was performed using Pearson's correlation coefficient.

For more details, see the [Supporting Materials and Methods](#) section.

Results

BILIARY PAUCITY, CHOLESTASIS, AND ABSENCE OF HEPATOCARCINOGENESIS IN IKK^{α/β}^{LPC-KO} ANIMALS ARE ASSOCIATED WITH NECROTIC AREAS AND ATTENUATED COMPENSATORY PROLIFERATION

Mice with conditional deletion of either *RelA/p65*, *Nemo*, or *Ikkα/Ikkβ* in LPCs show inhibition of the NF-κB pathway, but develop completely different spontaneous hepatic phenotypes.^(21–23) Though these findings suggested that NF-κB-independent functions might cause this paradox, these putative functions have not yet been resolved. To explore these putative functions, we focused on the specific phenotype caused by deletion of both catalytic subunits (*Ikkα* and *Ikkβ*) in LPCs (IKK^{α/β}^{LPC-KO}). As shown,⁽²²⁾ IKK^{α/β}^{LPC-KO} mice exhibited severe growth retardation and wasting attributed to cholestasis, compared to WT littermates or mice lacking *Nemo*, and most IKK^{α/β}^{LPC-KO} animals died within 7 months after birth. IKK^{α/β}^{LPC-KO} mice showed similarly elevated levels of the liver damage marker, alanine aminotransferase (ALT), compared to NEMO^{LPC-KO} mice. In contrast, IKK^{α/β}^{LPC-KO}, but not NEMO^{LPC-KO}, mice, revealed a massive elevation of the cholestasis indicator, serum bilirubin, and alkaline phosphatase (AP), which correlated with a reduction of intrahepatic bile ducts that was not visible in NEMO^{LPC-KO} mice ([Supporting Fig. S1A,B](#)). Therefore, IKK^{α/β} as well as NEMO prevent the development of spontaneous hepatitis, whereas only IKK^{α/β} but not NEMO prevent intrahepatic bile duct paucity and cholestasis.

Moreover, surviving 28- to 38-week-old $IKK\alpha/\beta^{LPC-KO}$ mice did not show any macroscopic sign of tumor development, whereas NEMOLPC-KO animals displayed multiple tumor nodules at the same age (Supporting Fig. S1C), illustrating that absence of *Ikk α* and *Ikk β* in LPC causes cholestasis, but not hepatocarcinogenesis.

Further analysis revealed that $IKK\alpha/\beta^{LPC-KO}$ and $NEMO^{LPC-KO}$ mice displayed similarly increased levels of cleaved CASPASE-3⁺ (cl. CASP-3⁺) in their livers (Supporting Fig. S1D). However, small areas of LPC necrosis were found in $IKK\alpha/\beta^{LPC-KO}$ livers that were not detected in $NEMO^{LPC-KO}$ livers (Supporting Fig. S1D). Compensatory LPC proliferation represents a fundamental cellular response toward cell death and drives hepatocarcinogenesis upon chronic injury.⁽²⁴⁾ In line with their high tumor load at older age, spontaneous LPC apoptosis correlated with strong compensatory LPC proliferation in $NEMO^{LPC-KO}$ mice, as shown by Ki67 staining (Supporting Fig. S1D). Surprisingly, in $IKK\alpha/\beta^{LPC-KO}$ mice, significantly less LPC were Ki-67 positive compared to $NEMO^{LPC-KO}$ livers (Supporting Fig. S1D). Of note, increased LPC apoptosis and proliferation in $NEMO^{LPC-KO}$ animals were not only detected in hepatocytes, but also cholangiocytes, as shown by double stainings for pan-cytokeratin (CK) and cl. CASP-3 as well as pan-CK and Ki-67, whereas similar double-positive cholangiocytes were not detected in $IKK\alpha/\beta^{LPC-KO}$ livers (Supporting Fig. S1E). Together, biliary paucity, cholestasis, and absence of hepatocarcinogenesis in $IKK\alpha/\beta^{LPC-KO}$ animals were associated with necrotic areas and attenuated compensatory cell proliferation.

RIPK3 IS ACTIVATED IN *Ikk α / β* -DEFICIENT LIVERS, BUT DOES NOT CONTROL CHOLESTASIS

Given that spontaneous necrotic areas were found in $IKK\alpha/\beta^{LPC-KO}$ livers and cholestasis was previously associated with RIPK3-dependent necroptosis in mice with ablation of *Tak1* in LPCs,⁽²⁵⁾ we wondered whether the necrotic areas in $IKK\alpha/\beta^{LPC-KO}$ livers reflected activation of RIPK3-dependent necroptosis.⁽²⁶⁾ In line with this hypothesis, western blotting analysis of RIPK3 expression in WT, $NEMO^{LPC-KO}$, and $IKK\alpha/\beta^{LPC-KO}$ livers revealed slightly elevated levels in $NEMO^{LPC-KO}$ mice, but a strikingly higher expression in $IKK\alpha/\beta^{LPC-KO}$ livers (Supporting Fig. S2A). Analysis of primary hepatocytes from $IKK\alpha/\beta^{LPC-KO}$ livers confirmed that up-regulation of RIPK3

expression occurred in LPCs and not in infiltrating hematopoietic cells (Supporting Fig. S2A). Moreover, purification of liver extracts with phospho-protein purification columns to enrich the phospho-proteome showed that mixed lineage kinase domain-like—the downstream mediator of necroptosis⁽²⁷⁾—was present in a phosphorylated state in $IKK\alpha/\beta^{LPC-KO}$, but not WT (Supporting Fig. S2B). Given that RIPK3 was attributed with necroptosis-independent functions, for example, in inflammasome activation,⁽²⁸⁾ we tested for cleavage of CASPASE-1 in liver extracts from the respective mouse lines, but could not detect a RIPK3-dependent regulation of CASPASE-1 cleavage in livers of $IKK\alpha/\beta^{LPC-KO}$ mice (Supporting Fig. S2C).

To assess whether RIPK3 mediated cholestasis in $IKK\alpha/\beta^{LPC-KO}$ livers, we generated mice with *Ikk α /Ikk β* deletion in LPCs and constitutive *Ripk3* deletion ($IKK\alpha/\beta^{LPC-KO}/RIPK3^{-/-}$) (Supporting Fig. S2D). Similarly to $IKK\alpha/\beta^{LPC-KO}$ mice, $IKK\alpha/\beta^{LPC-KO}/RIPK3^{-/-}$ animals displayed a severely reduced body weight and size as well as decreased liver sizes compared to WT animals, and most animals died within 7 months after birth (Fig. 1A-C). Moreover, serum analysis of ALT, bilirubin, and AP revealed similar levels between $IKK\alpha/\beta^{LPC-KO}/RIPK3^{-/-}$ and $IKK\alpha/\beta^{LPC-KO}$ 8-week-old mice (Fig. 1D), arguing against a rescue from cholestasis through additional *Ripk3* deletion. In line with this, quantification of pan-CK⁺ bile ducts demonstrated that $IKK\alpha/\beta^{LPC-KO}/RIPK3^{-/-}$ displayed biliary paucity to a similar extent as $IKK\alpha/\beta^{LPC-KO}$ animals (Fig. 1E). However, the amount of necrotic areas was significantly reduced upon additional *Ripk3* deletion (Fig. 1F). Together, these findings provide evidence that necroptosis is activated in LPCs of *Ikk α /Ikk β* -deficient livers, but it is not involved in the mediation of cholestasis in $IKK\alpha/\beta^{LPC-KO}$ mice.

AN RIPK3-INDEPENDENT FUNCTION OF RIPK1 PROMOTES CHOLESTASIS AND PREVENTS CARCINOGENESIS IN *IKK α / β* ^{LPC-KO} MICE

Although RIPK3 induces intrahepatic necrosis in $IKK\alpha/\beta^{LPC-KO}$ livers, cholestasis was not rescued by *Ripk3* deletion, suggesting an additional mediator involved in the biliary phenotype of $IKK\alpha/\beta^{LPC-KO}$ livers. The kinase, RIPK1, controls multiple pathways associated with programmed cell death.⁽²⁹⁾ We therefore hypothesized that RIPK1 might be involved in

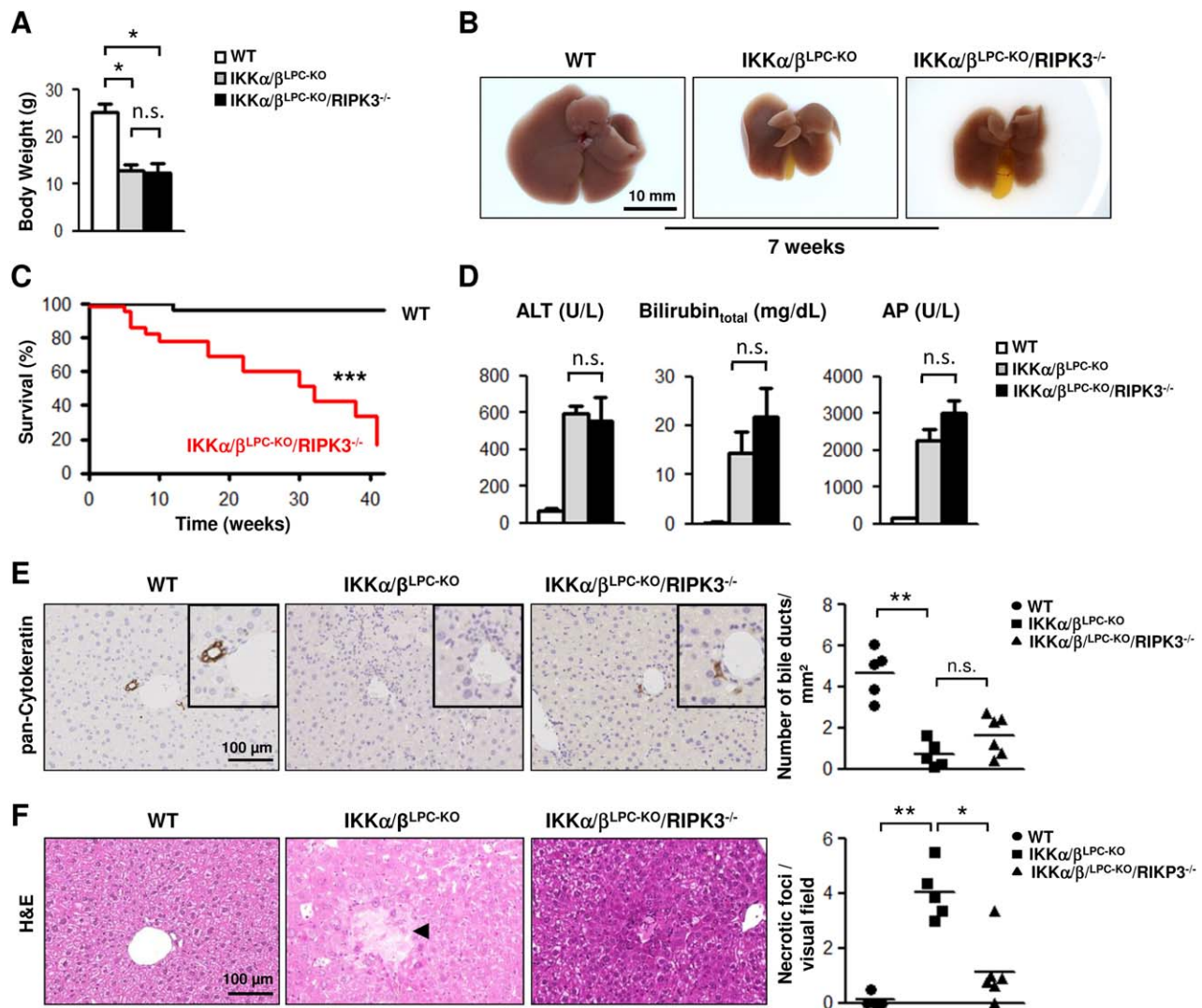


FIG. 1. *Ripk3* deletion in $IKK\alpha/\beta^{LPC-KO}$ livers reduces intrahepatic necrosis, but does not prevent cholestasis and reduction of intrahepatic bile ducts. (A) Body weight analysis of WT, $IKK\alpha/\beta^{LPC-KO}$, and $IKK\alpha/\beta^{LPC-KO}/RIPK3^{-/-}$ mice ($n = 4$). (B) Macroscopic appearance of representative livers of 7-week-old WT, $IKK\alpha/\beta^{LPC-KO}$, and $IKK\alpha/\beta^{LPC-KO}/RIPK3^{-/-}$ mice. (C) Kaplan-Meier curve showing spontaneous death of $IKK\alpha/\beta^{LPC-KO}/RIPK3^{-/-}$ mice between 5 and 42 weeks of age (WT, $n = 69$; $IKK\alpha/\beta^{LPC-KO}/RIPK3^{-/-}$, $n = 33$). (D) ALT, total serum bilirubin, and AP in 7- to 9-week-old WT, $IKK\alpha/\beta^{LPC-KO}$, and $IKK\alpha/\beta^{LPC-KO}/RIPK3^{-/-}$ mice ($n = 5$). (E) Immunohistochemistry and quantification of liver paraffin sections of WT, $IKK\alpha/\beta^{LPC-KO}$, and $IKK\alpha/\beta^{LPC-KO}/RIPK3^{-/-}$ mice for pan-CK⁺ bile ducts ($n = 5-6$). (F) H&E staining of liver paraffin sections of WT, $IKK\alpha/\beta^{LPC-KO}$, and $IKK\alpha/\beta^{LPC-KO}/RIPK3^{-/-}$ mice and quantification of necrotic foci ($n = 5-6$). Results are shown as mean; error bars denote SEM. * $P < 0.05$; ** $P < 0.01$; *** $P < 0.001$. Abbreviation: H&E, hematoxylin and eosin.

the mediation of the $IKK\alpha/\beta^{LPC-KO}$ phenotype and generated mice with combined LPC-specific deletion of *Ikk α* , *Ikk β* , and *Ripk1* ($IKK\alpha/\beta/RIPK1^{LPC-KO}$; Supporting Fig. S3A). Strikingly, $IKK\alpha/\beta/RIPK1^{LPC-KO}$ mice showed a normal body size and weight as well as normal liver sizes when compared to WT controls (Fig. 2A,B). Moreover, the earlier lethality of $IKK\alpha/\beta^{LPC-KO}$ and $IKK\alpha/\beta^{LPC-KO}/RIPK3^{-/-}$ mice was fully rescued

in $IKK\alpha/\beta/RIPK1^{LPC-KO}$ animals (Fig. 2C). On the serological level, $IKK\alpha/\beta/RIPK1^{LPC-KO}$ mice showed no reduction of ALT level (Fig. 2D), but they displayed a complete rescue from hyperbilirubinemia and strong reduction in AP levels as well as bile acid levels compared to $IKK\alpha/\beta^{LPC-KO}$ animals (Fig. 2D and Supporting Fig. S3B), coinciding with an increased number of bile ducts (Fig. 2E). Importantly, 3-week-old $IKK\alpha/\beta/RIPK1^{LPC-KO}$

$\beta^{\text{LPC-KO}}$ mice showed no significant impairment in bile duct formation compared to WT mice of the same age, and a reduction of small intrahepatic bile ducts started to occur in 5-week-old $\text{IKK}\alpha/\beta^{\text{LPC-KO}}$ mice, but not in $\text{IKK}\alpha/\beta/\text{RIPK1}^{\text{LPC-KO}}$ animals (Supporting Fig. S3C), arguing against a developmental defect underlying the biliary phenotype in 8-week-old animals. Of note, *Ripk1* deletion alone did not influence biliary homeostasis (Supporting Fig. S3D). We finally tested for the presence of liver tumors in older $\text{IKK}\alpha/\beta/\text{RIPK1}^{\text{LPC-KO}}$ mice and compared these to age- and sex-matched $\text{IKK}\alpha/\beta^{\text{LPC-KO}}$ animals. Older $\text{IKK}\alpha/\beta/\text{RIPK1}^{\text{LPC-KO}}$ animals developed small macroscopically visible nodules on their surfaces (Fig. 2F), corresponding to areas of increased proliferation and dysplasia on the histological level (Supporting Fig. S3E). In addition, 2 of 8 $\text{IKK}\alpha/\beta/\text{RIPK1}^{\text{LPC-KO}}$ animals (25%), but no age-matched $\text{IKK}\alpha/\beta^{\text{LPC-KO}}$ mice, showed at least one large liver tumor (Fig. 2F, marked by arrowhead), which on the histological level, corresponded to HCC (Supporting Fig. S3E). Together, these findings suggest that an NF- κ B- and RIPK3-independent function of RIPK1 mediates lethal cholestasis, but prevents tumorigenesis, in $\text{IKK}\alpha/\beta^{\text{LPC-KO}}$ animals.

***Ripk1* DELETION PROMOTES LPC PROLIFERATION AND ACCUMULATION OF γ -H2A.X⁺ LPC IN $\text{IKK}\alpha/\beta^{\text{LPC-KO}}$ MICE**

To define how RIPK1 mediated the phenotypes of $\text{IKK}\alpha/\beta^{\text{LPC-KO}}$ livers, we first tested the activation of apoptosis and necrosis in livers of 8-week-old $\text{IKK}\alpha/\beta/\text{RIPK1}^{\text{LPC-KO}}$ mice. As shown by histology, additional *Ripk1* deletion resulted in a marked decrease of necrotic foci, compared to $\text{IKK}\alpha/\beta^{\text{LPC-KO}}$ mice (Supporting Fig. S4A), which was already observed in 5-week-old, but not in 3-week-old, mice (Supporting Fig. S4B). Regarding apoptotic cell death, CASPASE-3 showed—if at all—a minimal, nonsignificant trend to lower cleavage levels upon additional *Ripk1* deletion at the examined time points as demonstrated by immunohistochemical staining (IHC) and western blotting analysis (Fig. 3A and Supporting Fig. S4C,D). These data provide evidence that RIPK1 is nonessential for the mediation of apoptosis, but necessary for the mediation of necrosis in *Ikk α* / *Ikk β* -deficient hepatocytes. Given that these cell-death analyses did not explain the differences in carcinogenesis and cholestasis between $\text{IKK}\alpha/\beta^{\text{LPC-KO}}$ and $\text{IKK}\alpha/\beta/\text{RIPK1}^{\text{LPC-KO}}$ animals, we hypothesized that a RIPK1-dependent inhibitory function on compensatory

cell proliferation might have caused organ hypotrophy (Fig. 2B), defective biliary regeneration leading to biliary paucity and cholestasis, as well as absence of cancer development in $\text{IKK}\alpha/\beta^{\text{LPC-KO}}$ mice. To test this, we stained young (3-, 5-, and 8-week-old) and older (26- to 40-week-old, age- and sex-matched) WT, $\text{IKK}\alpha/\beta^{\text{LPC-KO}}$, and $\text{IKK}\alpha/\beta/\text{RIPK1}^{\text{LPC-KO}}$ livers for Ki-67. Young $\text{IKK}\alpha/\beta/\text{RIPK1}^{\text{LPC-KO}}$ livers showed a trend to higher levels of Ki-67⁺ LPCs upon additional *Ripk1* deletion, whereas LPC proliferation was significantly higher in older $\text{IKK}\alpha/\beta/\text{RIPK1}^{\text{LPC-KO}}$ livers, compared to $\text{IKK}\alpha/\beta^{\text{LPC-KO}}$ mice, suggesting an antiproliferative function of RIPK1 in $\text{IKK}\alpha/\beta^{\text{LPC-KO}}$ mice (Fig. 3B and Supporting Fig. S4D). To further provide evidence for the functional relation between RIPK1, apoptosis, and compensatory proliferation in $\text{IKK}\alpha/\beta^{\text{LPC-KO}}$ mice, we performed a correlation analysis between cl. CASP-3⁺ and Ki-67⁺ LPCs as well as necrotic areas and Ki-67⁺ LPC in young mice (Fig. 3C). Interestingly, a significant positive correlation was detected between cl. CASP-3⁺ and Ki-67⁺ LPCs in $\text{IKK}\alpha/\beta/\text{RIPK1}^{\text{LPC-KO}}$ livers (Fig. 3C) and $\text{NEMO}^{\text{LPC-KO}}$ livers (Supporting Fig. S5), both of which develop liver cancer. In contrast, such a correlation was not observed in $\text{IKK}\alpha/\beta^{\text{LPC-KO}}$ mice (Fig. 3C). Moreover, none of the examined mouse livers showed a correlation between necrosis and Ki-67 positivity (Fig. 3C and Supporting Fig. S5).

Given the striking effects of *Ripk1* deletion on biliary cell homeostasis in $\text{IKK}\alpha/\beta^{\text{LPC-KO}}$ livers, we next analyzed expression of RIPK1, RIPK3, *IKK α* , *IKK β* , and *NEMO* in isolated and sorted CD326⁺ cells (cholangiocyte population⁽³⁰⁾) and compared it to the CD326⁻ fraction by quantitative real-time polymerase chain reaction (qRT-PCR). This analysis revealed no difference in expression levels of RIPK1, *IKK α* , and *IKK β* between both compartments, whereas RIPK3 expression was slightly decreased in the CD326⁺ fraction (Fig. 3D). In line with this, double staining of pan-CK and Ki-67 revealed proliferating bile duct cells in $\text{IKK}\alpha/\beta/\text{RIPK1}^{\text{LPC-KO}}$, but not in $\text{IKK}\alpha/\beta^{\text{LPC-KO}}$, livers (Fig. 3E), suggesting that similar regulatory mechanisms were activated in hepatocytes and cholangiocytes. Interestingly, we could detect some proliferating bile duct cells in 3-week-old WT, $\text{IKK}\alpha/\beta^{\text{LPC-KO}}$, and $\text{IKK}\alpha/\beta/\text{RIPK1}^{\text{LPC-KO}}$ mice, demonstrating normal development in all three genotypes (Supporting Fig. S4E, upper panel). However, immunohistological analysis of 5-week-old mice revealed some double-positive cells for pan-CK and Ki-67 only in $\text{IKK}\alpha/\beta/\text{RIPK1}^{\text{LPC-KO}}$ mice, but not in WT and $\text{IKK}\alpha/\beta^{\text{LPC-KO}}$ mice. Double

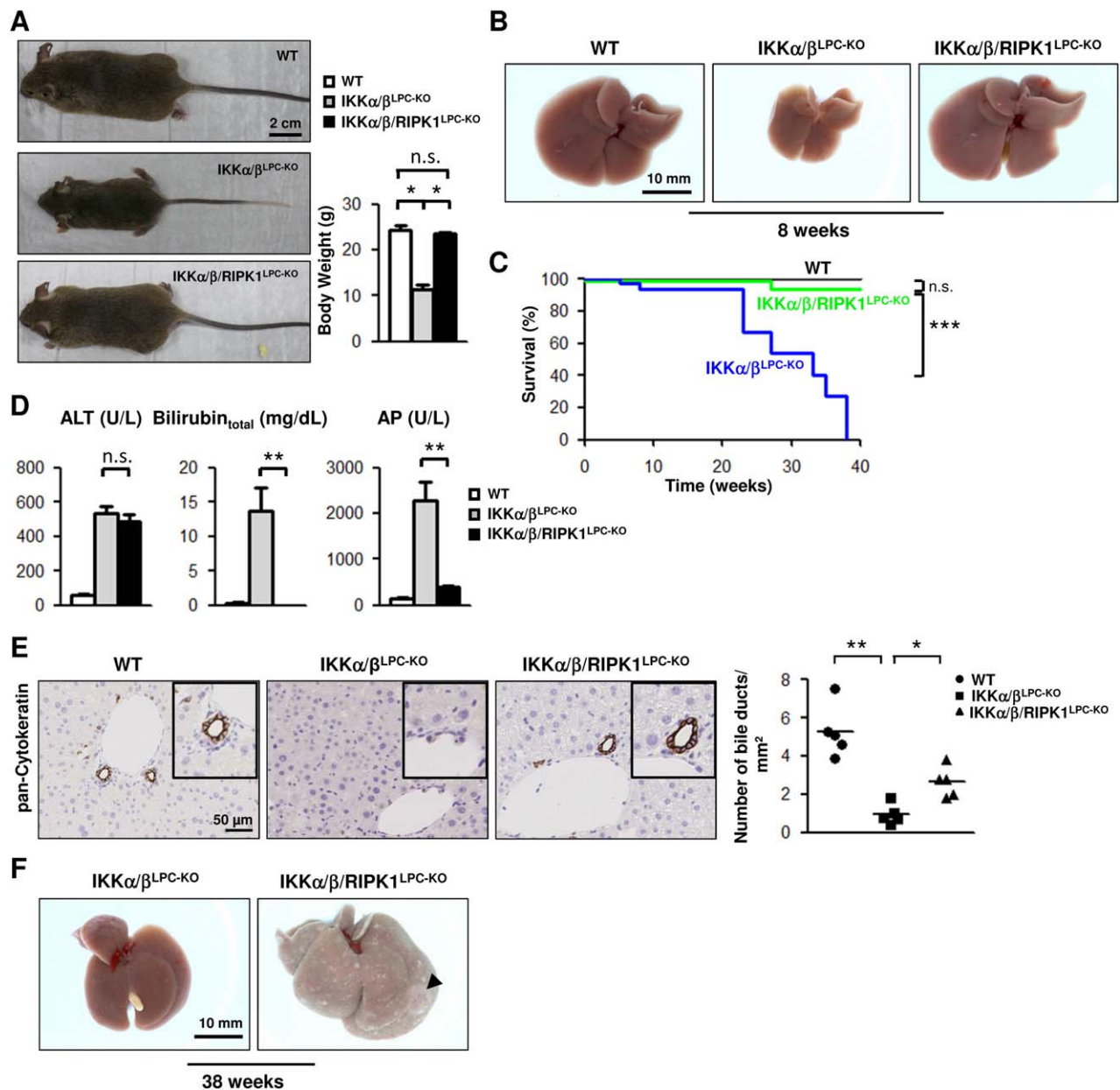


FIG. 2. RIPK1 promotes cholestasis and biliary paucity, but prevents tumorigenesis, in IKK α / β ^{LPC-KO} livers. (A) Representative macroscopic pictures of 8-week-old WT, IKK α / β ^{LPC-KO}, and IKK α / β /RIPK1^{LPC-KO} mice and body weight analysis (n = 4). (B) Representative pictures of 8-week-old WT, IKK α / β ^{LPC-KO}, and IKK α / β /RIPK1^{LPC-KO} livers. (C) Kaplan-Meier curve showing survival of WT, IKK α / β ^{LPC-KO}, and IKK α / β /RIPK1^{LPC-KO} mice until 42 weeks of age. (WT, n = 89; IKK α / β ^{LPC-KO}, n = 37; IKK α / β /RIPK1^{LPC-KO}, n = 51). (D) Serum-level analysis of ALT, total serum bilirubin, and AP in 7- to 9-week-old WT, IKK α / β ^{LPC-KO}, and IKK α / β /RIPK1^{LPC-KO} mice. (E) Pan-CK staining and statistical quantification of intrahepatic bile ducts on representative liver paraffin sections from WT, IKK α / β ^{LPC-KO}, and IKK α / β /RIPK1^{LPC-KO} mice (n = 5). (F) Representative macroscopic pictures of livers of 38-week-old IKK α / β ^{LPC-KO} and IKK α / β /RIPK1^{LPC-KO} mice. Results are shown as mean; error bars denote SEM. **P* < 0.05; ***P* < 0.01.

staining of liver tissue against pan-CK and cl. CASP-3 showed no apoptotic bile ducts cells in 3-week-old mice (Supporting Fig. S4E, lower panel). In contrast, we could detect double-positive cells for pan-CK and

cl. CASP-3 in 5-week-old IKK α / β ^{LPC-KO} and IKK α / β /RIPK1^{LPC-KO} mice, but not in WT mice. These data support our idea of an antiproliferative function of RIPK1. In 5-week-old IKK α / β ^{LPC-KO} mice, we

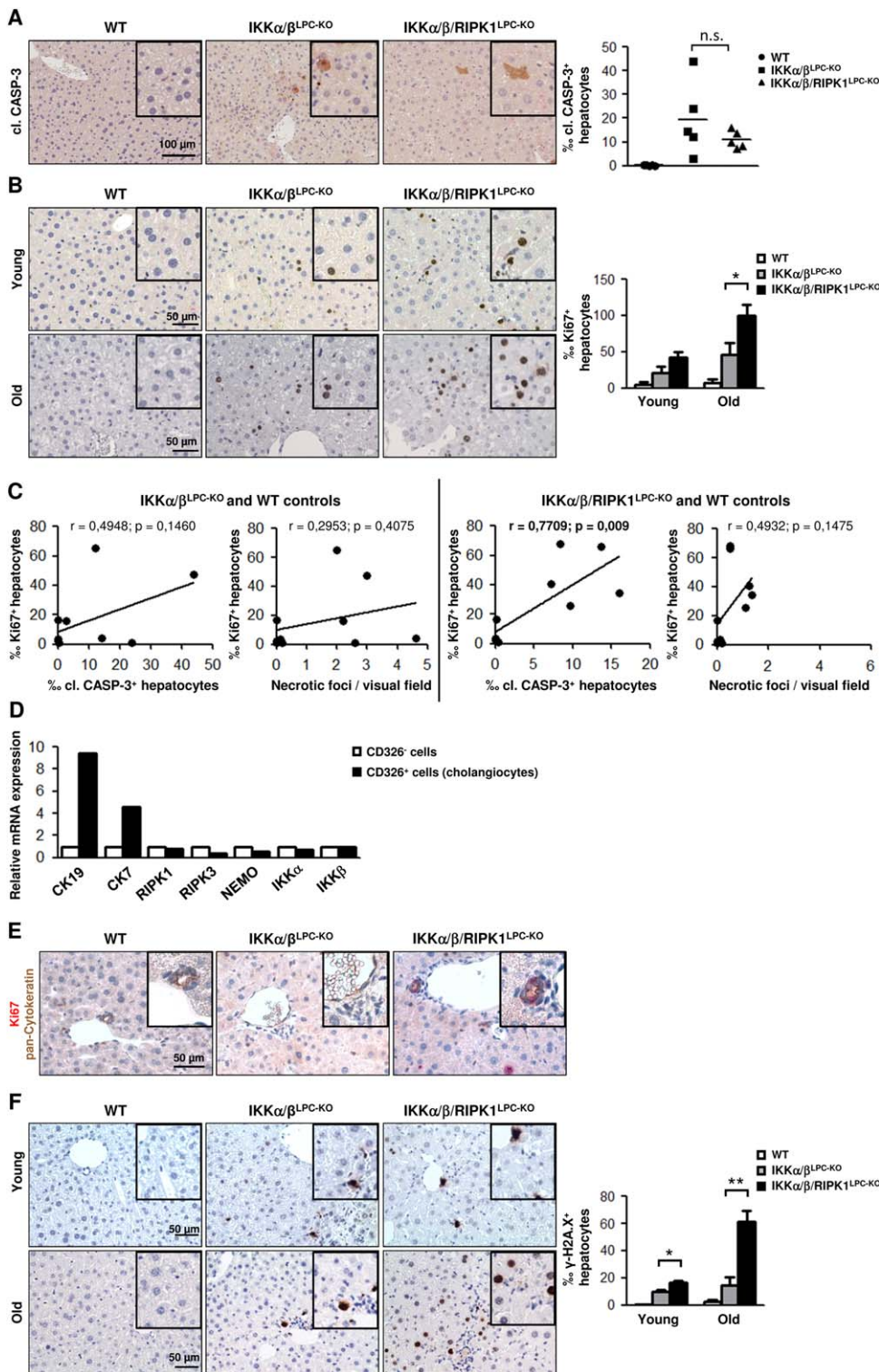


FIG. 3. RIPK1 inhibits compensatory LPC proliferation and accumulation of LPC with DNA damage in $IKK\alpha/\beta^{LPC-KO}$ mice. (A) Histological analysis and statistical quantification of cl. CASP-3⁺ LPCs in WT, $IKK\alpha/\beta^{LPC-KO}$, and $IKK\alpha/\beta/RIPK1^{LPC-KO}$ mice (n = 5). (B) Ki-67 staining and statistical quantification of representative liver paraffin sections from young (8-week-old) and older (26- to 40-week-old, age- and sex-matched) WT, $IKK\alpha/\beta^{LPC-KO}$, and $IKK\alpha/\beta/RIPK1^{LPC-KO}$ mice (n = 5). (C) Correlation analysis between Ki-67⁺ cells with cl. CASP-3⁺ cells or necrotic areas in liver tissue of the indicated genotypes was performed using Pearson's correlation coefficient. (D) Analysis of expression of indicated genes in CD326⁻ cells and CD326⁺ cells (cholangiocytes) by qRT-PCR. Combined values of two independent isolations. (E) Representative IHC of liver sections from WT, $IKK\alpha/\beta^{LPC-KO}$ and $IKK\alpha/\beta/RIPK1^{LPC-KO}$ mice (pan-CK is stained brown and Ki-67 is stained pink/red). (F) IHC and quantification of liver paraffin sections of indicated genotypes using a γ -H2A.X antibody (n = 5). Results are shown as mean; error bars denote SEM. **P* < 0.05; ***P* < 0.01. Abbreviation: n.s., not significant.

discovered apoptotic bile cells, but no compensatory proliferation, whereas we could detect both in 5-week-old $IKK\alpha/\beta/RIPK1^{LPC-KO}$ mice.

It was recently shown that RIPK1 maintains DNA integrity and that dysfunction of RIPK1 led to accumulation of lung cancer and MEF cells with increased

phosphorylation of H2A.X (γ -H2A.X),⁽³¹⁾ a widely used marker for DNA double-strand breaks and DNA damage and repair.^(32,33) In addition, it was shown that γ -H2A.X levels are increased in preneoplastic lesions of HCC.⁽³⁴⁾ In line with this, the number of γ -H2A.X⁺ LPCs was significantly higher in livers of young and old IKK α / β /RIPK1^{LPC-KO} mice, compared to IKK α / β ^{LPC-KO} animals (Fig. 3F). Together, these findings suggest that RIPK1 inhibits compensatory cell proliferation and accumulation of γ -H2A.X⁺ cells in livers of IKK α / β ^{LPC-KO} mice, thereby impeding carcinogenesis but promoting biliary paucity and cholestasis.

To exclude that additional *Ripk1* deletion reestablished activation of NF- κ B in IKK α / β ^{LPC-KO} mice, we performed western blotting analysis for I κ B α and electrophoretic mobility shift assay (EMSA) analysis, both of which confirmed that NF- κ B activation was similarly abolished in IKK α / β /RIPK1^{LPC-KO} mice (Supporting Fig. S6A,B). In line with this, qRT-PCR analysis showed similar expression levels of TNF α and interleukin-6 between IKK α / β ^{LPC-KO} mice and IKK α / β /RIPK1^{LPC-KO} mice (Supporting Fig. S6C), arguing against an NF- κ B-dependent effect on cytokine production driving the difference in compensatory LPC proliferation between the two mouse lines.

IKK α AND IKK β COLLABORATE IN MEDIATING CONSTITUTIVE PHOSPHORYLATION OF RIPK1 IN LPCs

Based on the fact that the RIPK1-dependent phenotype of cholestasis was only noted in IKK α / β ^{LPC-KO} mice, but not NEMO^{LPC-KO} animals, we hypothesized that it depended on the kinase function of the catalytic IKK subunits. To test this, we used an alternative approach to block catalytic IKK activity in the presence of NEMO and generated mice with conditional *Ikk β* -deletion in LPCs and constitutive expression of a kinase-dead mutant form of IKK α ⁽³⁵⁾ (IKK α ^{AA/AA}/IKK β ^{LPC-KO}). Coimmunoprecipitation experiments confirmed that the mutant IKK α ^{AA} form still bound to NEMO in IKK α ^{AA/AA}/IKK β ^{LPC-KO} livers, whereas—as expected—only free NEMO molecules were detected in IKK α / β ^{LPC-KO} animals (Fig. 4A). Of note, serological and histological examination revealed the presence of cholestasis, reduction of intrahepatic bile ducts, as well as presence of necrotic areas in IKK α ^{AA/AA}/IKK β ^{LPC-KO} livers (Fig. 4B-D). These findings support the hypothesis that the kinase

function of IKK subunits is required to suppress development of the spontaneous IKK α / β ^{LPC-KO} phenotype.

Based on the rescue of the NF- κ B-independent IKK α / β ^{LPC-KO} cholestasis phenotype through *Ripk1* deletion, we hypothesized that this phenotype was mediated through a kinase function of IKK α and IKK β targeting RIPK1. Of note, it was recently demonstrated that RIPK1 activation can be both positively and negatively regulated by phosphorylation,⁽³⁶⁾ suggesting that the catalytic IKKs might control RIPK1 activity by influencing its phosphorylation levels.

To test this, we specifically enriched the phosphoproteome in liver lysates from WT, IKK α / β ^{LPC-KO}, IKK α / β /RIPK1^{LPC-KO}, and NEMO^{LPC-KO} mice, followed by a western blotting analysis on these enriched lysates and control lysates using a standard antibody against RIPK1 (Fig. 5A). This analysis revealed a single RIPK1 band in phospho-enriched extracts of WT and NEMO^{LPC-KO} livers (Fig. 5A, left panel). In contrast, this signal was nearly absent in liver tissue of IKK α / β ^{LPC-KO} mice and completely vanished in IKK α / β /RIPK1^{LPC-KO} livers (Fig. 5A, right panel). This finding suggests that in WT and NEMO^{LPC-KO} livers in the resting state, IKK α and IKK β mediate constitutive phosphorylation of RIPK1. To confirm that the columns purify phosphorylated proteins, we treated the purified protein fraction of WT liver lysates with λ -protein phosphatase, resulting in enhanced mobility of RIPK1 on sodium dodecyl sulfate-polyacrylamide gel electrophoresis/western blotting analysis (Fig. 5B), providing further evidence for the specificity of this approach for detection of phosphorylated RIPK1 *in vivo*. We also could detect binding of IKK α / β to RIPK1 in WT and NEMO^{LPC-KO} mice 1 hour after stimulation with lipopolysaccharide (LPS), but not in IKK α / β IKK α / β /RIPK1^{LPC-KO} mice (Supporting Fig. S7A).

To further substantiate this hypothesis and test whether IKKs can directly phosphorylate RIPK1, we performed an *in vitro* kinase assay using a recombinant form of IKK α or IKK β , respectively, and an N-terminal fragment of RIPK1 containing the kinase domain as a substrate in the presence of the RIPK1 inhibitor, necrostatin 1 (Nec-1),⁽³⁷⁾ to prevent RIPK1 autophosphorylation. Addition of IKK α as well as IKK β induced strong *in vitro* phosphorylation of RIPK1 (Fig. 5C). To identify specific IKK-dependent phosphorylation sites in RIPK1, we immunoprecipitated RIPK1 from RIPK1/hemagglutinin (HA)/green fluorescent protein (GFP)-transfected human hepatoma cells (HepG2) as well as HEK 293T cells treated with or without the IKK inhibitor, thiophenecarboxamide (TPCA-1), and performed a mass spectrometry analysis. We could repeatedly identify Serine

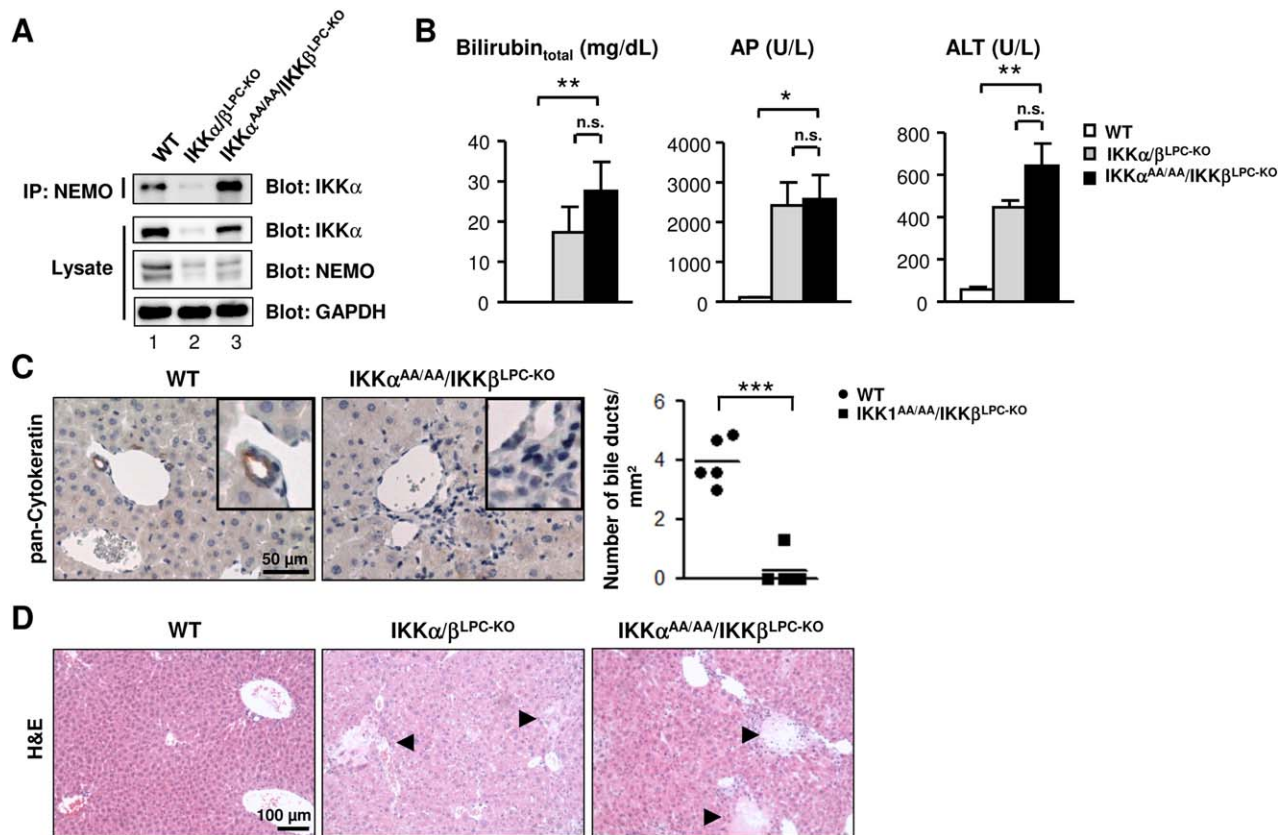


FIG. 4. IKK α ^{AA/AA}/IKK β ^{LPC-KO} mice show intrahepatic bile duct paucity and cholestasis. (A) Immunoprecipitation of NEMO from livers of WT, IKK α / β ^{LPC-KO}, and IKK α ^{AA/AA}/IKK β ^{LPC-KO} mice and western blotting analysis for the presence of IKK α . Lysates were analyzed as indicated. (B) Serum level analysis of total bilirubin, AP, and ALT in male mice (n = 5). (C) Pan-CK staining and statistical quantification of intrahepatic bile ducts on representative liver paraffin sections from WT and IKK α ^{AA/AA}/IKK β ^{LPC-KO} mice (n = 5). (D) Representative H&E staining of liver paraffin sections of WT, IKK α / β ^{LPC-KO}, and IKK α ^{AA/AA}/IKK β ^{LPC-KO} mice. Results are shown as mean; error bars denote SEM. **P* < 0.05; ***P* < 0.01; ****P* < 0.001. Abbreviations: H&E, hematoxylin and eosin; n.s., not significant.

320, Serine 330/331 (ambiguous phosphorylation site identification attributed to neighboring Serine residues), and Serine 416 as phosphorylated residues in RIPK1 in both cell lines (Fig. 5D). In contrast to Serine 330/331 and Serine 416, Serine 320 was not found to significantly change its phosphorylation status in a TPCA-1-dependent manner. Based on this finding and the fact that Serine 330/331 had previously been identified as a phosphorylation site not modified by autophosphorylation,^(36,38) we decided to generate a Serine 330/331 to alanine mutant (RIPK1_{S330/331A}-HA-GFP). Mutant (RIPK1_{S330/331A}-HA-GFP) or WT RIPK1 (RIPK1-HA-GFP), respectively, were transfected into hepatoma cells and cell viability was assessed by a methyl thiazol tetrazolium (MTT) proliferation assay, which revealed a decreased cell viability upon mutant RIPK1 transfection (Fig. 5E,F). Of note,

additional TPCA treatment of mutant RIPK1 transfected cells resulted in an even further viability reduction (Supporting Fig. S7B), suggesting that also other phospho-acceptor sites in RIPK1 exist controlling cell viability. Taken together, these findings suggest that RIPK1 is a direct phosphorylation target of the catalytic IKK subunits, transmitting a previously unrecognized IKK-dependent signal controlling cell viability and proliferation, cancer development, and biliary homeostasis.

RIPK1 EXPRESSION IS DOWN-REGULATED IN A SUBGROUP OF HUMAN HCC

The previous findings suggested that, under certain circumstances, RIPK1 might exert an antiproliferative

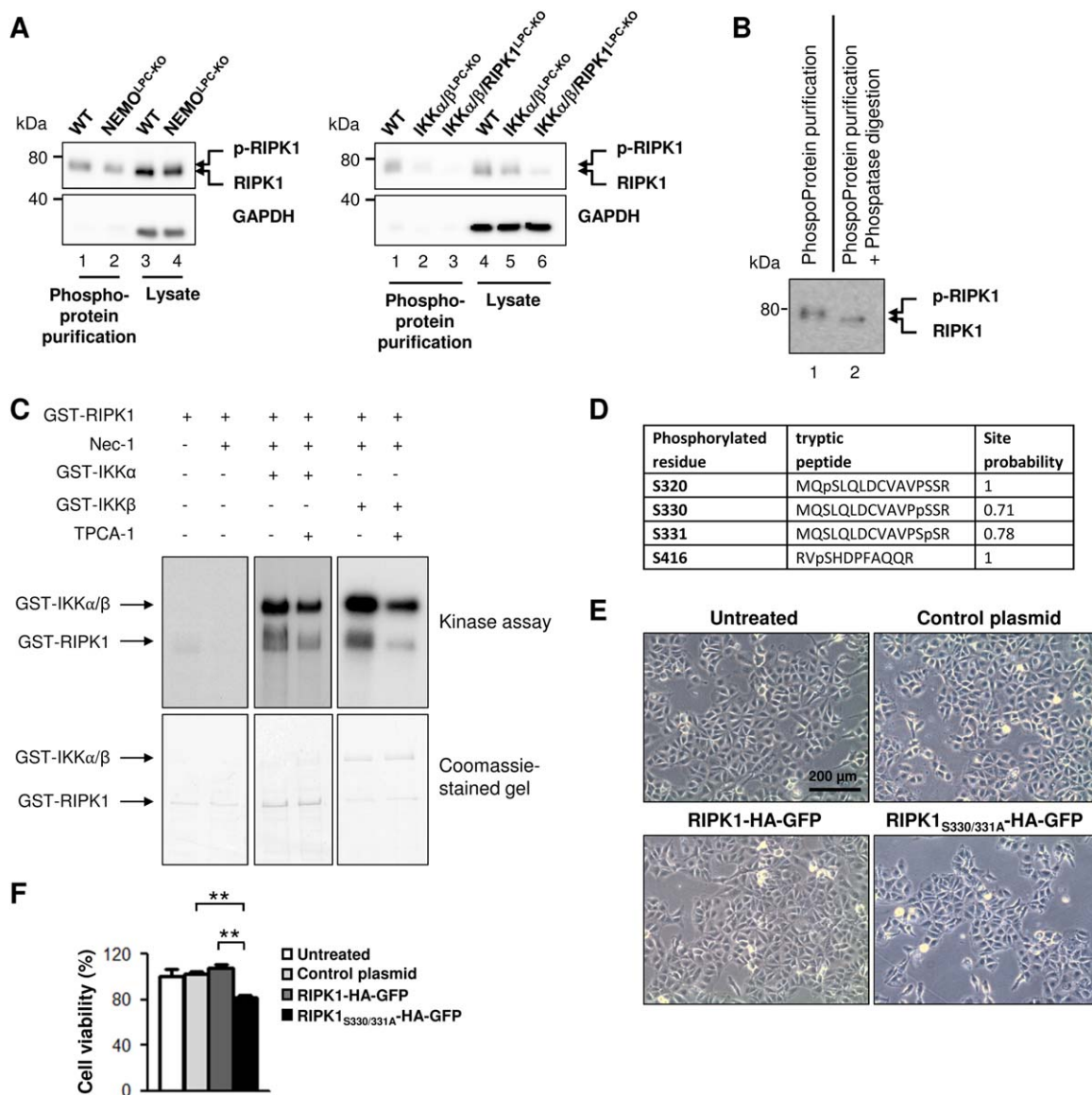


FIG. 5. IKK α and IKK β mediate RIPK1 phosphorylation in LPCs. (A) Purification of phosphorylated proteins from livers of the indicated genotypes and analysis by western blotting. Lysates were analyzed as indicated. (B) Purification of phosphorylated proteins from livers of WT without (1) or with λ -phosphatase treatment (2). (C) *In vitro* kinase assays with a recombinant form of human IKK α or IKK β , respectively, and an N-terminal fragment of RIPK1 containing the kinase domain as substrate. Kinase reaction was performed in the presence of the RIPK1-inhibitor, Nec-1, to prevent RIPK1 autophosphorylation. Moreover, reactions were preincubated with the IKK inhibitor, TPCA-1, as indicated. (D) Phosphorylated peptides repeatedly identified in RIPK1-HA-GFP immunoprecipitated from transfected cells using nano liquid chromatography tandem mass spectrometry LC-MS/MS as described in the Materials and Methods section. Because of a rather low phosphorylation site probability, Serine 330/331 identification remains ambiguous, whereas the other two sites show a 100% localization probability. (E) Representative pictures of Hu7 cells 24 hours after transfection with control plasmid (empty backbone), RIPK1-HA-GFP, or RIPK1_{S330/331A}-HA-GFP as well as untreated cells. (F) Analysis of cell viability of transfected Hu7 cells (E) by MTT assay. Results are expressed as mean from three replicate cultures. Results are shown as mean; error bars denote SEM. ***P* < 0.01. Abbreviation: GST, glutathione δ -transferase.

function in hepatocytes with implications for hepatocarcinogenesis. Thus, we performed an explorative analysis of RIPK1 expression in a small collective of human HCCs. For this, we compared protein

expression in liver needle biopsies and resection samples of 19 individual treatment-naïve human HCCs (Supporting Fig. S8A; Supporting Table S1) with tissue from control patients without chronic liver disease.

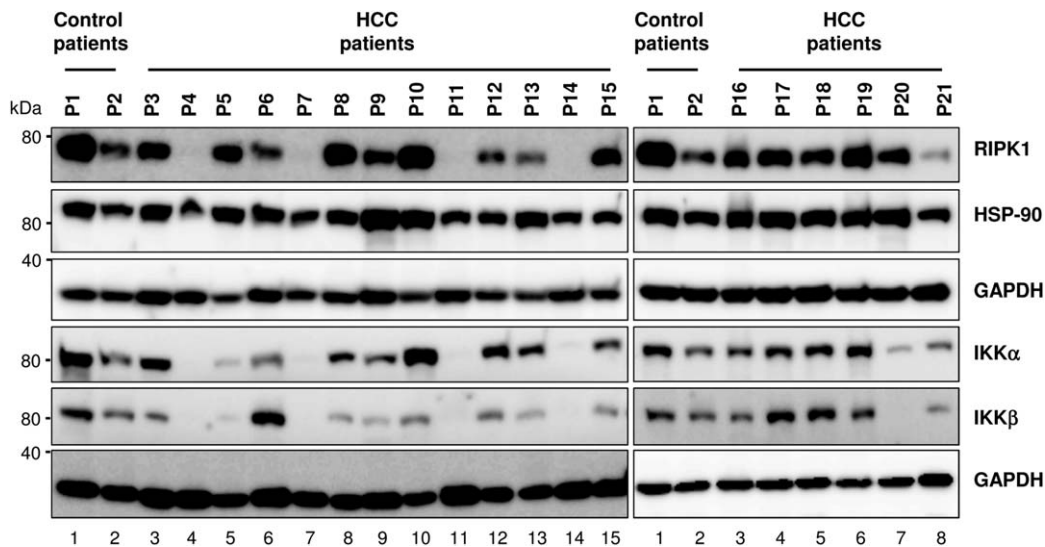


FIG. 6. Variable RIPK1 expression in human HCCs. Expression analysis on protein lysates from human HCC specimens and control tissue from patients without primary liver tumors. Western blotting analysis was performed using antibodies against RIPK1, IKK α , and IKK β , HSP-90 and GAPDH served as loading control (control patients without chronic liver disease, P1, P2; HCC patients, P3-P21).

These western blotting analyses revealed a variable expression of RIPK1, IKK α , and IKK β in human HCC compared with a rather uniform expression of heat shock protein 90 (HSP-90), a highly abundant chaperon used as a control, as well as glyceraldehyde-3-phosphate dehydrogenase (GAPDH; Fig. 6). Of note, 5 of 19 HCC (P4, P7, P11, P14, and P21) showed a strong reduction in RIPK1, IKK α , and IKK β expression (Fig. 6). In these tumors, neither a specific disease entity nor a specific histological subtype could be clearly attributed to the subgroup of RIPK1- and IKK-deficient HCC (Supporting Table S1; Supporting Fig. S7). These provide initial evidence that the tumor-suppressive function of RIPK1 shown here might be of relevance in a presently undefined subgroup of HCC patients, requiring further confirmation in a larger cohort of HCC patients.

Discussion

The IKK complex was regarded as part of a linear signaling cascade mediating activation of the canonical and/or noncanonical NF- κ B pathways.⁽³⁹⁾ Previous *in vivo* studies examining the function of NF- κ B in liver cancer by targeting different molecules in the NF- κ B pathway led to controversial results, which, until now,

could not be resolved.⁽⁴⁰⁾ Recently, several studies provided compelling evidence that IKK subunits might control important cellular functions like cell death, independently of NF- κ B.^(4,5) This suggested that contradicting findings on the functions of IKK subunits and NF- κ B in liver cancer might, at least in part, be explained by previously unrecognized, NF- κ B-independent functions of IKK subunits.⁽⁴⁰⁾ Here, we show that the catalytic IKK subunits, IKK α and IKK β , regulate different RIPK1-dependent pathways that control intrahepatic programmed necrosis, hepatocarcinogenesis, and cholestasis. In addition, we provide evidence that this regulation might be exerted through direct phosphorylation of RIPK1 (see Fig. 7).

It was shown previously that activation of RIPK1 can be both negatively and positively regulated by phosphorylation.⁽³⁶⁾ Here, we provide evidence that RIPK1 is constitutively phosphorylated by IKK α /IKK β in the liver, an organ that is constantly challenged by stimuli transmitted from the gut microbiome.^(41,42) In human hepatoma cells and HEK 293T cells, we could identify two IKK-dependent phosphorylation sites, Serine 330/331 and Serine 416, which could be down-regulated by treatment with the IKK-inhibitor, TPCA-1. Interestingly, these two sites that we identified in TPCA-1-treated cultured cells were recently also found in an *in vitro* experimental

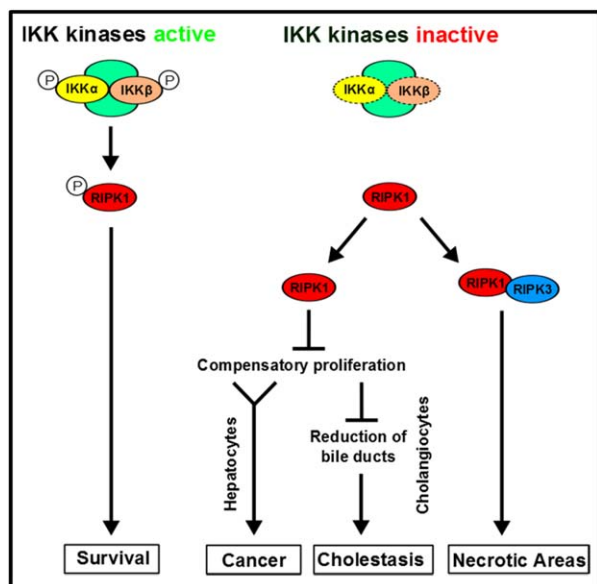


FIG. 7. Model for RIPK1-dependent functions in $IKK\alpha/\beta$ -deficient livers. Schematic model of RIPK1-dependent functions spontaneously activated upon combined deletion or inhibition of the two $I\kappa B$ -Kinase subunits, $IKK\alpha$ and $IKK\beta$.

setting.⁽⁴³⁾ supporting our hypothesis that these sites are specifically regulated by IKKs. At present, it is unclear whether $IKK\alpha$ and $IKK\beta$ redundantly target these respective sites *in vivo* or whether $IKK\alpha$ and $IKK\beta$ target specific sites in RIPK1. Moreover, it remains to be determined whether additional phospho-acceptor sites are directly or indirectly targeted by $I\kappa B$ -Kinase *in vivo*, which were not detected in our cell-culture approach using (potentially less effective) chemical IKK inhibition instead of genetic targeting. In this context, it is important to note that we could not precipitate endogenous RIPK1 efficiently enough from murine liver lysates to perform MS, mass spectrometry analysis (data not shown). Endogenous TAP-tagging of RIPK1 in mouse liver could be an efficient approach to solve this problem. Importantly, whereas NEMO is considered essential for activation of $I\kappa B\alpha$ -directed activity of the IKK complex in response to TNF stimulation,⁽²¹⁾ it was previously shown that $IKK\alpha$ and $IKK\beta$ can constitutively phosphorylate the NF- κB subunit, p65, in liver cells independently of the presence of NEMO.⁽²²⁾ In this line of thought, our present data provide further evidence that $I\kappa B\alpha$ -independent kinase functions of the IKK complex can be constitutively active independently of NEMO.

In contrast to $IKK\alpha/\beta/RIPK1^{LPC-KO}$ mice, animals with conditional deletion of the RelA/p65 subunits neither develop any spontaneous apoptosis nor liver cancer.^(22,23) This difference to the $IKK\alpha/\beta/RIPK1^{LPC-KO}$ phenotype might be explained by the formation and nuclear translocation of RelA/p65-independent NF- κB dimers in RelA conditional knockouts, providing a level of NF- κB activity that prevents spontaneous activation of complex IIA and apoptosis. Next to complex IIA, a complex, IIB, was previously described mediating CASPASE-3-dependent apoptosis depending on RIPK1, FADD, and CASPASE-8.^(10,11) Our present findings suggested that this pathway did not contribute significantly to the spontaneous phenotype observed in $IKK\alpha/\beta^{LPC-KO}$ mice. However, it was previously shown that mice with conditional $Ikk\alpha/Ikk\beta$ deletion in LPCs develop massive liver failure and show even more CASPASE-3 cleavage than livers with *Nemo* deletion in LPC upon stimulation with bacterial LPS, an inducer of internal TNF secretion.⁽²²⁾ Thus, it is possible that complex IIB containing RIPK1 might contribute to LPC apoptosis upon LPS/TNF stimulation rather than to spontaneous apoptosis in $IKK\alpha/\beta^{LPC-KO}$ mice.

In addition to their role in NF- κB activation, we show here that $IKK\alpha$ and $IKK\beta$ suppress spontaneous activation of RIPK1-dependent pathways with distinct biological outcomes (Fig. 7). First, $IKK\alpha/\beta^{LPC-KO}$ mice developed focal intrahepatic necrosis areas in an RIPK3-dependent fashion (Fig. 1F). Whereas it seemed to be an established concept that necroptosis depends on the formation of RIPK1/RIPK3 dimers,^(7,8) it was recently suggested that RIPK1 might not mediate, but rather inhibit, necroptosis in gut or skin epithelial cells.⁽⁴⁴⁾ Our present data that $IKK\alpha/\beta/RIPK1^{LPC-KO}$ mice showed a strong reduction in necrosis, compared to $IKK\alpha/\beta^{LPC-KO}$ mice, argue for an essential role of RIPK1 in liver cells.

Finally, our data suggest that RIPK1 in $IKK\alpha/\beta^{LPC-KO}$ mice controlled a response pathway to apoptosis that inhibited the accumulation of γ -H2A.X⁺ LPCs and compensatory LPC proliferation, ultimately preventing carcinogenesis but promoting biliary paucity and cholestasis (Fig. 7). Moreover, the effects of RIPK1 on compensatory proliferation were moderate and clearer in older mice. Of note, tumor incidence in $IKK\alpha/\beta/RIPK1^{LPC-KO}$ mice was lower than previously shown for NEMO^{LPC-KO} animals, who have a 100% tumor penetrance.⁽¹⁵⁾ This is most likely attributed to the fact that apoptosis and carcinogenesis in

NEMO^{LPC-KO} animals also relies on complex IIB that contains RIPK1⁽⁴⁵⁾ and is therefore not functional in hepatocytes of IKK α / β /RIPK1^{LPC-KO} mice.

Interestingly, biliary paucity and lethal cholestasis in IKK α / β ^{LPC-KO} mice strictly correlated with the presence of RIPK1, but not RIPK3. Our findings on defective proliferation rates of RIPK1-competent IKK α / β ^{LPC-KO} livers, together with the fact that young NEMO^{LPC-KO} mice show a strong ductular reaction and expansion of oval cells to maintain biliary integrity in a context of chronic inflammation,⁽¹⁵⁾ suggest that an insufficient biliary regeneration attributed to the presence of (hypophosphorylated) RIPK1 is the main reason for biliary paucity in IKK α / β ^{LPC-KO} livers. Interestingly, it was previously shown that RIPK1 and Jun-(N)-terminal kinase 1 can mediate necrosis of cells by inducing mitochondrial dysfunction.⁽⁴⁶⁾ Therefore, we can presently not exclude that some IKK-deficient biliary cells might preferentially undergo RIPK1-dependent cell death, contributing to the net decrease of biliary cells in IKK α / β ^{LPC-KO} livers.

In conclusion, our data provide evidence that IKK α and IKK β control different RIPK1-dependent signaling pathways controlling liver cancer and biliary homeostasis as fundamental consequences of chronic hepatic inflammation. A better understanding of these RIPK1-dependent pathways might lead to novel pharmacological strategies in patients with chronic liver disease, liver cancer, and cholestasis.

Acknowledgments: We express our gratitude to Yinling Hu (NIH, Bethesda, MD) for kindly providing IKK α ^{F1} mice. We thank Jacqueline Döntgen, Carmen Tag, Sibille Sauer-Lehnen, and Barbara Lippok for excellent technical assistance.

REFERENCES

- 1) Bruix J, Sherman M; American Association for the Study of Liver Diseases. Management of hepatocellular carcinoma: an update. HEPATOLOGY 2011;53:1020-1022.
- 2) Ben-Neriah Y, Karin M. Inflammation meets cancer, with NF-kappaB as the matchmaker. Nat Immunol 2011;12:715-723.
- 3) Hacker H, Karin M. Regulation and function of IKK and IKK-related kinases. Sci STKE 2006;2006:re13.
- 4) Yan J, Xiang J, Lin Y, Ma J, Zhang J, Zhang H, et al. Inactivation of BAD by IKK inhibits TNF α -induced apoptosis independently of NF- κ B activation. Cell 2013;152:304-315.
- 5) Baldwin AS. Regulation of cell death and autophagy by IKK and NF- κ B: critical mechanisms in immune function and cancer. Immunol Rev 2012;246:327-345.
- 6) Ofengeim D, Yuan J. Regulation of RIP1 kinase signalling at the crossroads of inflammation and cell death. Nat Rev Mol Cell Biol 2013;14:727-736.
- 7) Vandenebeele P, Declercq W, Van Herreweghe F, Vanden Berghe T. The role of the kinases RIP1 and RIP3 in TNF-induced necrosis. Sci Signal 2010;3:re4.
- 8) Cho YS, Challa S, Moquin D, Genga R, Ray TD, Guildford M, Chan FK. Phosphorylation-driven assembly of the RIP1-RIP3 complex regulates programmed necrosis and virus-induced inflammation. Cell 2009;137:1112-1123.
- 9) He S, Wang L, Miao L, Wang T, Du F, Zhao L, Wang X. Receptor interacting protein kinase-3 determines cellular necrotic response to TNF- α . Cell 2009;137:1100-1111.
- 10) Dickens LS, Powley IR, Hughes MA, MacFarlane M. The 'complexities' of life and death: death receptor signalling platforms. Exp Cell Res 2012;318:1269-1277.
- 11) Wilson NS, Dixit V, Ashkenazi A. Death receptor signal transducers: nodes of coordination in immune signaling networks. Nat Immunol 2009;10:348-355.
- 12) Dara L, Johnson H, Suda J, Win S, Gaarde W, Han D, Kaplowitz N. Receptor interacting protein kinase 1 mediates murine acetaminophen toxicity independent of the necrosome and not through necroptosis. HEPATOLOGY 2015;62:1847-1857.
- 13) Cox J, Mann M. MaxQuant enables high peptide identification rates, individualized p.p.b.-range mass accuracies and proteome-wide protein quantification. Nat Biotechnol 2008;26:1367-1372.
- 14) Jouan-Lanhouet S, Arshad MI, Piquet-Pellorce C, Martin-Chouly C, Le Moigne-Muller G, Van Herreweghe F, et al. TRAIL induces necroptosis involving RIPK1/RIPK3-dependent PARP-1 activation. Cell Death Differ 2012;19:2003-2014.
- 15) **Bettermann K, Vucur M**, Haybaeck J, Koppe C, Janssen J, Heymann F, et al. TAK1 suppresses a NEMO-dependent but NF-kappaB-independent pathway to liver cancer. Cancer Cell 2010;17:481-496.
- 16) Liu B, Xia X, Zhu F, Park E, Carbajal S, Kiguchi K, et al. IKK α is required to maintain skin homeostasis and prevent skin cancer. Cancer Cell 2008;14:212-225.
- 17) Maeda S, Kamata H, Luo JL, Leffert H, Karin M. IKK β couples hepatocyte death to cytokine-driven compensatory proliferation that promotes chemical hepatocarcinogenesis. Cell 2005;121:977-990.
- 18) Kellendonk C, Opherk C, Anlag K, Schutz G, Tronche F. Hepatocyte-specific expression of Cre recombinase. Genesis 2000;26:151-153.
- 19) Senftleben U, Cao Y, Xiao G, Greten FR, Krähn G, Bonizzi G, et al. Activation by IKK α of a second, evolutionary conserved, NF-kappa B signaling pathway. Science 2001;293:1495-1499.
- 20) Newton K, Sun X, Dixit VM. Kinase RIP3 is dispensable for normal NF-kappa Bs, signaling by the B-cell and T-cell receptors, tumor necrosis factor receptor 1, and Toll-like receptors 2 and 4. Mol Cell Biol 2004;24:1464-1469.
- 21) Luedde T, Beraza N, Kotsikoris V, van Loo G, Nenci A, De Vos R, et al. Deletion of NEMO/IKKgamma in liver parenchymal cells causes steatohepatitis and hepatocellular carcinoma. Cancer Cell 2007;11:119-132.
- 22) Luedde T, Heinrichsdorff J, De Lorenzi R, De Vos R, Roskams T, Pasparakis M. IKK1 and IKK2 cooperate to maintain bile duct integrity in the liver. Proc Natl Acad Sci U S A 2008;105:9733-9738.
- 23) Geisler F, Algul H, Paxian S, Schmid RM. Genetic inactivation of RelA/p65 sensitizes adult mouse hepatocytes to TNF-induced apoptosis in vivo and in vitro. Gastroenterology 2007;132:2489-2503.

- 24) Luedde T, Kaplowitz N, Schwabe RF. Cell death and cell death responses in liver disease: mechanisms and clinical relevance. *Gastroenterology* 2014;147:765-783.e4.
- 25) **Vucur M, Reisinger F, Gautheron J**, Janssen J, Roderburg C, Cardenas DV, et al. RIP3 inhibits inflammatory hepatocarcinogenesis but promotes cholestasis by controlling caspase-8- and JNK-dependent compensatory cell proliferation. *Cell Rep* 2013;4:776-790.
- 26) Vanden Berghe T, Linkermann A, Jouan-Lanhouet S, Walczak H, Vandenabeele P. Regulated necrosis: the expanding network of non-apoptotic cell death pathways. *Nat Rev Mol Cell Biol* 2014;15:135-147.
- 27) Wang H, Sun L, Su L, Rizo J, Liu L, Wang LF, et al. Mixed lineage kinase domain-like protein MLKL causes necrotic membrane disruption upon phosphorylation by RIP3. *Mol Cell* 2014;54:133-146.
- 28) Weng D, Marty-Roix R, Ganesan S, Proulx MK, Vladimer GI, Kaiser WJ, et al. Caspase-8 and RIP kinases regulate bacteria-induced innate immune responses and cell death. *Proc Natl Acad Sci U S A* 2014;111:7391-7396.
- 29) Weinlich R, Green DR. The two faces of receptor interacting protein kinase-1. *Mol Cell* 2014;56:469-480.
- 30) Azimifar SB, Nagaraj N, Cox J, Mann M. Cell-type-resolved quantitative proteomics of murine liver. *Cell Metab* 2014;20:1076-1087.
- 31) Chen W, Wang Q, Bai L, Chen W, Wang X, Tellez CS, et al. RIP1 maintains DNA integrity and cell proliferation by regulating PGC-1 α -mediated mitochondrial oxidative phosphorylation and glycolysis. *Cell Death Differ* 2014;21:1061-1070.
- 32) Mah LJ, El-Osta A, Karagiannis TC. γ H2AX: a sensitive molecular marker of DNA damage and repair. *Leukemia* 2010;24:679-686.
- 33) Burma S, Chen BP, Murphy M, Kurimasa A, Chen DJ. ATM phosphorylates histone H2AX in response to DNA double-strand breaks. *J Biol Chem* 2001;276:42462-42467.
- 34) Matsuda Y, Wakai T, Kubota M, Osawa M, Takamura M, Yamagiwa S, et al. DNA damage sensor γ -H2AX is increased in preneoplastic lesions of hepatocellular carcinoma. *ScientificWorldJournal* 2013;2013:597095.
- 35) Cao Y, Bonizzi G, Seagroves TN, Gretchen FR, Johnson R, Schmidt EV, Karin M. IKK α provides an essential link between RANK signaling and cyclin D1 expression during mammary gland development. *Cell* 2001;107:763-775.
- 36) **McQuade T, Cho Y**, Chan FK. Positive and negative phosphorylation regulates RIP1- and RIP3-induced programmed necrosis. *Biochem J* 2013;456:409-415.
- 37) **Takahashi N, Duprez L**, Grootjans S, Cauwels A, Nerinckx W, DuHadaway JB, et al. Necrostatin-1 analogues: critical issues on the specificity, activity and in vivo use in experimental disease models. *Cell Death Dis* 2012;3:e437.
- 38) Degterev A, Hitomi J, Gemscheid M, Ch'en IL, Korkina O, Teng X, et al. Identification of RIP1 kinase as a specific cellular target of necrostatins. *Nat Chem Biol* 2008;4:313-321.
- 39) Hayden MS, Ghosh S. Signaling to NF- κ B. *Genes Dev* 2004;18:2195-2224.
- 40) Vainer GW, Pikarsky E, Ben-Neriah Y. Contradictory functions of NF- κ B in liver physiology and cancer. *Cancer Lett* 2008;267:182-188.
- 41) **Dapito DH, Mencin A, Gwak GY, Pradere JP**, Jang MK, Mederacke I, et al. Promotion of hepatocellular carcinoma by the intestinal microbiota and TLR4. *Cancer Cell* 2012;21:504-516.
- 42) Schwabe RF, Jobin C. The microbiome and cancer. *Nat Rev Cancer* 2013;13:800-812.
- 43) Dondelinger Y, Jouan-Lanhouet S, Divert T, Theatre E, Bertin J, Gough PJ, et al. NF- κ B-independent role of IKK α /IKK β in preventing RIPK1 kinase-dependent apoptotic and necroptotic cell death during TNF signaling. *Mol Cell* 2015;60:63-76.
- 44) **Dannappel M, Vlantis K, Kumari S, Polykratis A**, Kim C, Wachsmuth L, et al. RIPK1 maintains epithelial homeostasis by inhibiting apoptosis and necroptosis. *Nature* 2014;513:90-94.
- 45) **Kondylis V, Polykratis A**, Ehlken H, Ochoa-Callejero L, Straub BK, Krishna-Subramanian S, et al. NEMO prevents steatohepatitis and hepatocellular carcinoma by inhibiting RIPK1 kinase activity-mediated hepatocyte apoptosis. *Cancer Cell* 2015;28:582-598.
- 46) Xu Y, Huang S, Liu ZG, Han J. Poly(ADP-ribose) polymerase-1 signaling to mitochondria in necrotic cell death requires RIP1/TRAF2-mediated JNK1 activation. *J Biol Chem* 2006;281:8788-8795.

Author names in bold designate shared co-first authorship.

Supporting Information

Additional Supporting Information may be found at onlinelibrary.wiley.com/doi/10.1002/hep.28723/supinfo.